Physics Letters B 753 (2016) 586–590

Contents lists available at ScienceDirect

Physics Letters B

www.elsevier.com/locate/physletb

Thermal dileptons as fireball thermometer and chronometer

Ralf Rapp [a], Hendrik van Hees [b,c,*]

[a] Cyclotron Institute and Department of Physics and Astronomy, Texas A&M University, College Station, TX 77843-3366, USA
[b] Institut für Theoretische Physik, Johann-Wolfgang-Goethe-Universität Frankfurt, Max-von-Laue-Str. 1, D-60438 Frankfurt, Germany
[c] Frankfurt Institute for Advanced Studies, Ruth-Moufang-Str. 1, D-60438 Frankfurt, Germany

ARTICLE INFO

Article history:
Received 14 July 2015
Received in revised form 11 December 2015
Accepted 22 December 2015
Available online 29 December 2015
Editor: J.-P. Blaizot

ABSTRACT

Thermal dilepton radiation from the hot fireballs created in high-energy heavy-ion collisions provides unique insights into the properties of the produced medium. We first show how the predictions of hadronic many-body theory for a melting ρ meson, coupled with quark–gluon plasma emission utilizing a modern lattice-QCD based equation of state, yield a quantitative description of dilepton spectra in heavy-ion collisions at the SPS and the RHIC beam energy scan program. We utilize these results to systematically extract the excess yields and their invariant-mass spectral slopes to predict the excitation function of fireball lifetimes and (early) temperatures, respectively. We thereby demonstrate that future measurements of these quantities can yield unprecedented information on basic fireball properties. Specifically, our predictions quantify the relation between the measured and maximal fireball temperature, and the proportionality of excess yield and total lifetime. This information can serve as a "caloric" curve to search for a first-order QCD phase transition, and to detect non-monotonous lifetime variations possibly related to critical phenomena.

Collisions of heavy nuclei at high energies enable the creation of hot and dense strongly interacting matter, not unlike the one that filled the Universe during its first few microseconds. While the primordial medium was characterized by a nearly vanishing net baryon density (at baryon chemical potential $\mu_B \simeq 0$), heavy-ion collisions can effectively vary the chemical potential by changing the beam energy, thus facilitating systematic investigations of large parts of the phase diagram of Quantum Chromodynamics (QCD). The yields and transverse-momentum (p_T) spectra of produced hadrons have been widely used to determine the conditions of the fireball at chemical and kinetic freeze-out, to infer its properties when the hadrons decouple. Electromagnetic radiation (photons and dileptons), on the other hand, is emitted throughout the evolution of the expanding fireball with negligible final-state interactions and thus, in principle, probes the earlier hotter phases of the medium [1]. In particular, dilepton invariant-mass spectra have long been recognized as the only observable which gives direct access to an in-medium spectral function of the QCD medium, most notably of the ρ meson [2–5]. They also allow for a temperature measurement which is neither distorted by blue-shift effects due to collective expansion (as is the case for p_T spectra of hadrons and photons), nor limited by the hadron formation temperature [6]. For example, recent theoretical calculations of thermal photon spectra [7–9] exhibit the importance of blue-shift effects in extracting the average temperature. In particular, they illustrate that the inverse slope parameter of $T_{\rm slope} \simeq 240$ MeV extracted by the PHENIX Collaboration from direct photons in Au–Au($\sqrt{s_{\rm NN}} = 200$ GeV) collisions at RHIC [10] corresponds to emission temperatures over a broad window around $T_{\rm pc} \simeq 160$ MeV; this interpretation is corroborated by the observation of a large elliptic flow. On the other hand, even at the lower energies of the SPS, (Lorentz-) *invariant*-mass dilepton spectra for $M > 1$ GeV, which are not subject to blue-shift effects, reveal an average temperature significantly above $T_{\rm pc}$ (see below).

Significant excess radiation of dileptons in ultrarelativistic heavy-ion collisions (URHICs), beyond final-state hadron decays, was established at the CERN-SPS program, at collision energies of $\sqrt{s_{NN}} \simeq 17.3$ GeV [11,12]. The excess was found to be consistent with thermal radiation from a locally equilibrated fireball [13,14], with the low-mass spectra requiring substantial medium effects on the ρ line shape. The SPS dilepton program culminated in the high-precision NA60 data [12], which quantitatively confirmed the melting of the ρ resonance and realized the long-sought thermometer at masses $M > 1$ GeV. The extracted temperature amounts to $T = 205 \pm 12$ MeV, which probes relatively early phases in the fireball evolution, thereby significantly exceeding the pseudo-critical temperature computed in thermal lattice-QCD

* Corresponding author at: Institut für Theoretische Physik, Johann-Wolfgang-Goethe-Universität Frankfurt, Max-von-Laue-Str. 1, D-60438 Frankfurt, Germany.
E-mail address: hees@fias.uni-frankfurt.de (H. van Hees).

http://dx.doi.org/10.1016/j.physletb.2015.12.065

(lQCD), $T_{\rm pc} = 150$–170 MeV [15]. With the spectral shape under control, the magnitude of low-mass excess radiation enabled an unprecedented extraction of the fireball lifetime, $\tau_{\rm fb} = 7 \pm 1$ fm/c.

In the present letter, based on a robust description of existing dilepton data at the SPS and RHIC, we show that temperature and lifetime measurements through intermediate- and low-mass dileptons are a quantitative tool to characterize the fireballs formed in heavy-ion collisions. We predict pertinent excitation functions over a large range in center-of-mass energy, $\sqrt{s_{NN}} \simeq 6$–200 GeV. Related earlier work on this topic can be found, *e.g.*, in Refs. [16–18]. The motivation for the present study is strengthened by several recent developments. First, we show that the implementation of a modern lQCD equation of state (EoS) into the fireball evolution of In–In collisions at SPS recovers an accurate description of the NA60 excess data over the entire mass range, thus superseding earlier results with a first-order transition [19]. Second, the predictions of this framework turn out to agree well with the low-mass dilepton data from the STAR beam-energy scan-I (BES-I) campaign [20–22], in Au–Au collisions from SPS to top RHIC energies, at $\sqrt{s_{NN}} = 19.6, 27, 39, 62.4$ and 200 GeV [23]. Third, a recent implementation of the in-medium ρ spectral function into coarse-grained UrQMD transport calculations yields excellent agreement with both NA60 data and HADES data from SIS-18 in Ar–KCl($\sqrt{s_{NN}} = 2.6$ GeV) reactions [24,25] (the former agree well with the fireball calculations); and fourth, several future experiments (CBM, NA60+, NICA, STAR BES-II) plan precision measurements of dilepton spectra in the energy regime of $\sqrt{s_{NN}} \simeq 5$–20 GeV [26], where the fireball medium is expected to reach maximal baryon density and possibly come close to a critical point in the QCD phase diagram [27]. Our predictions thus provide a baseline for fundamental, but hitherto undetermined properties of the fireball, allowing for accurate tests of our understanding of these. In turn, marked deviations of upcoming data from the theoretical predictions will help discover new phenomena that induce unexpected structures in the lifetime and/or temperature excitation functions.

Let us recall the basic elements figuring into our calculation of dilepton excess spectra in URHICs. We assume local thermal equilibrium of the fluid elements in an expanding fireball, after a (short) initial equilibration period. The thermal radiation of dileptons is obtained from the differential production rate per unit four-volume and four-momentum [28–30],

$$\frac{{\rm d}N_{ll}}{{\rm d}^4x{\rm d}^4q} = -\frac{\alpha^2}{3\pi^3}\frac{L(M)}{M^2}\ {\rm Im}\,\Pi^{\mu}_{{\rm EM},\mu}(M,q)\ f_{\rm B}(q_0;T), \tag{1}$$

with $f_{\rm B}(q_0;T)$: thermal Bose function, $\alpha = \frac{e^2}{4\pi} \simeq \frac{1}{137}$: electromagnetic (EM) coupling constant, $L(M)$: final-state lepton phase space factor, and $M = \sqrt{q_0^2 - q^2}$: dilepton invariant mass (q_0: energy, q: three-momentum in the local rest frame of the medium). The EM spectral function, ${\rm Im}\,\Pi_{\rm EM}$, is well known in the vacuum, being proportional to the cross section for $e^+e^- \to$ hadrons. In the low-mass region (LMR), $M \leq 1$ GeV, it is saturated by the light vector mesons ρ, ω and ϕ, while the intermediate-mass region (IMR), $M \geq 1.5$ GeV, is characterized by a quark–antiquark continuum which hadronizes into multi-meson states.

Medium effects on the EM spectral function are calculated as follows. In hadronic matter the vector-meson propagators are computed in many-body theory based on effective Lagrangians with parameters constrained by vacuum scattering and resonance decay data [31,13,32]. The resulting ρ spectral function strongly broadens and melts toward the phase transition region (similar for the ω, which, however, contributes less than 10% to the dilepton yield; the ϕ is assumed to decouple near $T_{\rm pc}$ and does not produce thermal hadronic emission). For masses $M \geq 1$ GeV, we include emission due to multi-pion annihilation using a continuum extracted from vacuum τ-decay data, augmented with medium effects due to chiral mixing [33,34,19]. For emission from the quark–gluon plasma (QGP), we employ an lQCD-motivated rate [23] fitted to M-dependent spectral functions above $T_{\rm pc}$ [35,36] and supplemented by a finite-q dependence taken from perturbative photon rates [37]. The resulting QGP rates are quite similar to hard-thermal-loop results [38] and to next-to-leading order perturbative calculations carried down to $M, q \simeq \pi T$ [39]. The QGP and in-medium hadronic rates are nearly degenerate at temperatures around ~ 170 MeV.

To obtain dilepton spectra in URHICs, the rates need to be integrated over the space–time evolution of the collision. As in our previous work [19,7,23,9], we employ a simplified model in terms of an isentropically expanding thermal fireball. Its radial and elliptic flow are parameterized akin to hydrodynamic models and fitted to observed bulk-particle spectra and elliptic flow (π, K, p) at kinetic freeze-out, $T_{\rm kin} \simeq 100$–120 MeV, and to multistrange hadron observables (*e.g.*, ϕ) at chemical freeze-out, $T_{\rm ch} \simeq 160$ MeV. The kinetic freeze-out temperatures and radial flow velocities are in accordance with systematic blast-wave analyses of bulk-hadron spectra from SPS, RHIC and LHC [40]. The key link of the fireball expansion to dilepton emission is the underlying EoS, which converts the time-dependent entropy density, $s(\tau) = S/V_{\rm fb}(\tau) \equiv s(T(\tau), \mu_{\rm B}(\tau))$ ($V_{\rm fb}$: fireball volume), into temperature and chemical potential. We employ the EoS constructed in Ref. [41], where a parameterization of the $\mu_{\rm B} = 0$ lQCD results for the QGP [42,43] has been matched to a hadron resonance gas (HRG) at $T_{\rm pc} = 170$ MeV, with subsequent hadro-chemical freeze-out at $T_{\rm ch} = 160$ MeV. We here extend this construction to finite $\mu_{\rm B} = 3\mu_q$ with guidance from lQCD: The pseudo-critical temperature is reduced as $T_{\rm pc}(\mu_q) = T_{\rm pc}[1 - 0.08(\mu_q/T_{\rm pc})^2]$ [44,45], and the $\mu_q = 0$ parameterization of the QGP entropy density, $s(T, \mu_q = 0)$, is augmented by a quadratic correction as

$$s(\mu_q, T) = s(T, 0)[1 + c(\mu_q/\pi T)^2]\,. \tag{2}$$

Here, the coefficient c encodes the non-perturbative effects ($c \simeq 1$ in the perturbative limit); it has been numerically adjusted to best reproduce the finite-μ_q entropy densities plotted in Refs. [46,47] over the relevant temperature ranges. This yields $c \simeq 7$ for the conditions at $\sqrt{s_{\rm NN}} = 6.27$ GeV and 8.77 GeV, and $c \simeq 3.5$ for $\sqrt{s_{\rm NN}} = 20$ GeV. The small μ_q values at 62.4 GeV and 200 GeV render $s(\mu_q, T)$ insensitive to c; we have smoothly interpolated it to $c \simeq 1.5$ for $\mu_q \to 0$ which corresponds to its lQCD value of $c = 18\pi^2 c_2/4c_0$ when neglecting their temperature derivatives and higher coefficients (using the notation of Ref. [47] for the μ_B-expansion coefficients, c_n). It turns out that the fitted value of $c \simeq 7$ at the two lowest energies leads to a continuous entropy density across $T_{\rm pc}$ from the HRG to lQCD EoS. We can therefore only estimate an uncertainty by increasing c (otherwise the entropy density of the HRG would exceed the one for the QGP at $T_{\rm pc}$); we will investigate the impact of a 50% increase corresponding to the upper end of the error bars of the lQCD entropy densities. This increase creates a short-lived mixed phase of duration $\Delta\tau_{\rm mix} \simeq 0.7$ fm/c in the fireball evolution at $\sqrt{s_{\rm NN}} = 6.27$ GeV and 8.77 GeV. For the HRG EoS, we adopt the chemical freeze-out parameters of Ref. [48] as listed in Table 1.

As in hydrodynamic models, we need to specify the initial size of the fireball which in turn determines the initial temperature, T_0. The initial transverse radius is estimated from a standard Glauber model, while the larger uncertainty resides in the longitudinal size, z_0. In the high-energy limit of Bjorken expansion, it is related to the usual formation time via $\tau_0 = z_0\Delta y$ where $\Delta y \simeq 1.8$ corresponds to the rapidity width of the thermal fireball. At RHIC energies we adopt values used in our previous work [23], $\tau_0 \simeq 1/3$

Table 1
Excitation function of fireball parameters for its initial longitudinal size (z_0) and temperature (T_0), equation of state (T_{pc}), and chemical/kinetic freeze-out (T_{ch}, μ_B^{ch}, T_{kin}) conditions.

$\sqrt{s}$ (GeV)	6.3	8.8	19.6	62.4	200
z_0 (fm/c)	2.1	1.87	1.41	0.94	0.63
T_0 (MeV)	185	198	238	291	363
T_{pc} (MeV)	161	163	170	170	170
T_{ch} (MeV)	134	148	160	160	160
μ_B^{ch} (MeV)	460	390	197	62	22
T_{kin} (MeV)	114	113	111	108	104

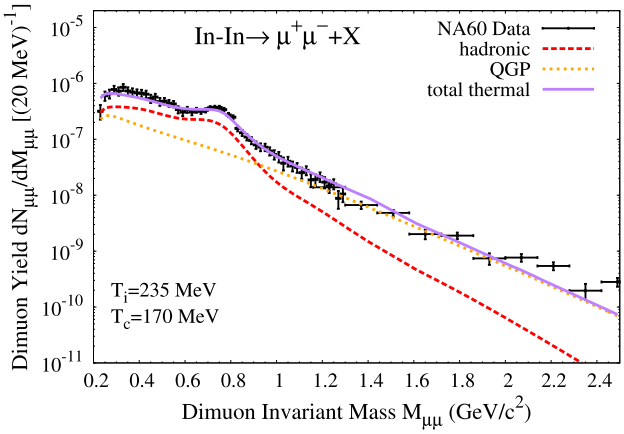

Fig. 1. (Color online.) Excess dimuon invariant-mass spectra in In–In($\sqrt{s_{NN}}$ = 17.3 GeV) collisions at the SPS. Theoretical calculations (solid line), composed of hadronic radiation (using in-medium ρ and ω spectral functions and multi-pion annihilation with chiral mixing, dashed line) and QGP radiation (using a lattice-QCD inspired rate, dotted line) are compared to NA60 data [49,12].

(1/2) at 200 (62.4) GeV. At top SPS energy ($\sqrt{s_{NN}} \simeq 20$ GeV) we use $\tau_0 \simeq 0.8$ fm/c which is slightly smaller than the "standard" value of 1 fm/c employed in Ref. [19], mainly to better describe the NA60 IMR spectra while staying above the nuclear overlap time of $R_A/\gamma = 0.7$ fm/c (which may be considered a lower limit for thermalization). We then extrapolated these values to lower energies with a power-law fit $z_0 = 4(\sqrt{s_{NN}})^{-0.35}$, resulting in the quoted values for $\sqrt{s_{NN}} = 8.77$ GeV and 6.27 GeV. At these energies, a relation between τ_0 and z_0 is no longer meaningful. Rather, one can compare the initial energy densities obtained from our z_0 values to transport calculations, cf., *e.g.*, Fig. 6.2 in part III of "The CBM physics book" [26] (page 638). For example, for $E_{lab} = 20$ GeV (corresponding to $\sqrt{s_{NN}} = 6.27$ GeV) various dynamical models produce a maximal excitation energy density (in the center of the collision) of $\epsilon^*_{max} = 1.6$–2.4 GeV/fm^3, compared to an average $\epsilon_0 = 1.6$ GeV/fm^3 in our fireball for $z_0 = 2.1$ fm. This appears to be a reasonable match, but we will consider a range of a factor of ~ 2 by varying z_0 by $\pm 30\%$.

We first test our updated approach with the most precise dilepton data to date, the acceptance-corrected NA60 excess dimuons in In–In($\sqrt{s_{NN}} = 17.3$ GeV) collisions [49,12], cf. Fig. 1. Good agreement with the invariant-mass spectrum is found, which also holds for the q_t dependence, as well as for CERES data [50] (not shown). This confirms our earlier conclusions that the ρ-meson melts around T_{pc} [19], while the IMR is dominated by radiation from above T_{pc} [51–54], mostly as a consequence of a non-perturbative EoS [55]. Our predictions for low-mass and q_t spectra of the RHIC BES-I program [23] also agree well with STAR [20–22] and the revised PHENIX [56] dielectron data. This framework therefore provides a robust interpretation of dilepton production in URHICs in terms of thermal radiation. In the following we utilize this set-up to extract the excitation function of two key fireball properties, *i.e.*, its total lifetime and an average (early) temperature, directly from

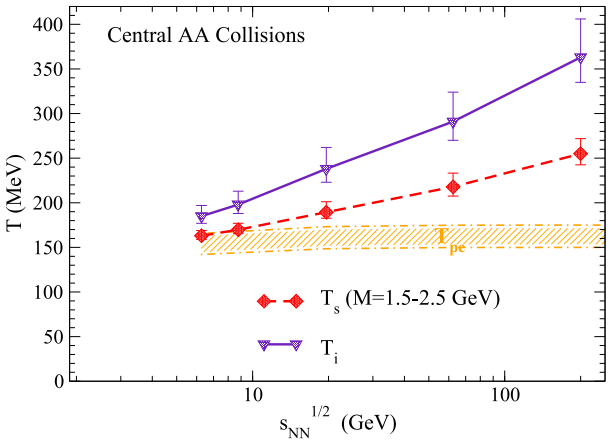

Fig. 2. (Color online.) Excitation function of the inverse-slope parameter, T_s, from intermediate-mass dilepton spectra ($M = 1.5$–2.5 GeV, diamonds connected with dashed line) and initial temperature T_0 (triangles connected with solid line) in central heavy-ion collisions ($A \simeq 200$). The error bars on T_s and T_0 correspond to a variation in the initial longitudinal fireball size, z_0, by $\pm 30\%$ around the central values quoted in Table 1. The hatched area schematically indicates the pseudo-critical temperature regime at vanishing (and small) chemical potential as extracted from various quantities computed in lattice QCD [15].

suitably chosen invariant-mass spectra. This should not merely be viewed as a prediction, but rather serve as a baseline to possibly discover effects indicative of new physics.

For the temperature determination we utilize the IMR, where medium effects on the EM spectral function are parametrically small, of order T^2/M^2, providing a stable thermometer. With $\mathrm{Im}\,\Pi_{EM} \propto M^2$, and in nonrelativistic approximation, one obtains

$$\mathrm{d}R_{ll}/\mathrm{d}M \propto (MT)^{3/2} \exp(-M/T)\,, \tag{3}$$

which is *independent* of the medium's collective flow, *i.e.*, there are no blue-shift effects. The observed spectra necessarily involve an average over the fireball evolution, but the choice of mass window, 1.5 GeV $\leq M \leq$ 2.5 GeV, implies $T \ll M$ and therefore much enhances the sensitivity to the early high-T phases of the evolution. Since primordial (and pre-equilibrium) contributions are not expected to be of exponential shape (*e.g.*, power law for Drell–Yan), their "contamination" may be judged by the fit quality of the exponential ansatz. The inverse slopes, T_s, extracted from the thermal radiation as computed above are displayed in Fig. 2 for collision energies of $\sqrt{s_{NN}} = 6$–200 GeV. We find a smooth dependence ranging from $T \simeq 160$ MeV to 260 MeV. The latter value unambiguously indicates that a thermalized QGP with temperatures well above the pseudo-critical one has been produced. Our results furthermore quantify that the "measured" average temperature at top RHIC energy is about 30% below the corresponding initial one (T_0). This gap significantly decreases when lowering the collision energy, to less than 15% at $\sqrt{s_{NN}} = 6$ GeV. This is in large part a consequence of the (pseudo-) latent heat in the transition which needs to be burned off in the expansion/cooling. The collision energy range below $\sqrt{s_{NN}} = 10$ GeV thus appears to be well suited to map out this transition regime and possibly discover a plateau in the IMR dilepton slopes akin to a "caloric curve". Another benefit at these energies is the smallness of the open-charm contribution (not included here), so that its subtraction does not create a large systematic error in the thermal-slope measurement (at higher energies, especially at RHIC and LHC, the open-charm and -bottom contributions to the IMR dilepton spectra become large and need to be carefully assessed to extract the thermal signal, ideally by both theoretical modeling of heavy-flavor diffusion/energy loss and experimental techniques such as displaced vertices or electron–

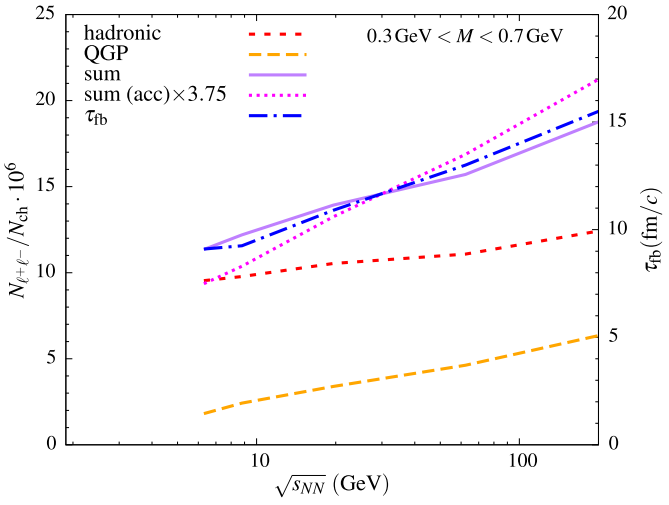

Fig. 3. (Color online.) Excitation function of low-mass thermal dilepton radiation ("excess spectra") in 0–10% central AA collisions ($A \simeq 200$), integrated over the mass range $M = 0.3$ GeV–0.7 GeV, for QGP (dashed line) and in-medium hadronic (short-dashed line) emission and their sum (solid line). The underlying fireball lifetime (dot-dashed line) is given by the right vertical scale.

muon correlations; these efforts are ongoing but beyond the scope of the current work).

Let us elaborate on some of the uncertainties in our predictions for the average temperature extracted from the IMR dilepton slopes. The largest one is associated with the assumed initial longitudinal fireball size, z_0. Varying the default values quoted in Table 1 by ±30% induces a ∼ 3–7% change in the extracted slopes, and a somewhat larger change for the initial temperatures (represented by the error bars in Fig. 2). At given $\sqrt{s}$, the ratio $T_{\rm s}/T_0$ is stable within less than 5%. A smaller error is given by the uncertainty of the QGP rate in the IMR. Replacing the QGP-motivated rate by the $q\bar{q}$ Born rate gives virtually identical results, while the use of the HTL rate [38] affects the extracted slopes by around 1%. Finally, we evaluated the uncertainty in our construction of the μ_q dependence of the equation of state. Not surprisingly, it is largest at the lowest collision energy: when increasing c from 7 to 10.5, the extracted slope parameter at $\sqrt{s_{\rm NN}} = 6.3$ GeV decreases by 2.3% (from 163 to 159.3 MeV), which is less than from the variation in z_0 (and not included in the error bars in Fig. 2). This uncertainty rapidly decreases with increasing collision energy, due to the decreasing c and μ_q values.

We finally investigate the relation between the fireball lifetime and the thermal dilepton yields, integrated over a suitable mass window. In Fig. 3 we display the results for a window below the free ρ/ω mass, which is often used to characterize the low-mass excess radiation. It turns out that the integrated thermal excess radiation tracks the total fireball lifetime remarkably well, within less than 10%. An important reason for this is that, despite the dominantly hadronic contribution, the QGP one is still significant. The latter would be relatively more suppressed when including the ρ/ω peak region. Likewise, the hadronic medium effects are essential to provide sufficient yield in the low-mass region; in particular, the baryon density effects on the ρ spectral function cause a ∼ 50% larger enhancement (relative to emission based on a vacuum spectral function) at $\sqrt{s_{\rm NN}} = 6.3$ GeV compared to 200 GeV. We have checked that, when hadronic medium effects are neglected, or when the mass window is extended, the proportionality of the excess yield to the lifetime is compromised. The impact of variations in the initialization of the fireball are rather small: varying z_0 by ±30% leads to a ca. ±3% variation in the low-mass yield at $\sqrt{s_{\rm NN}} = 6.3$ GeV for a fixed lifetime, and much less at collider energies (*e.g.*, ±0.5% at 62.4 GeV). Variations in the coefficient c of the entropy density lead to negligible effects on the low-mass yields at fixed lifetime (due to a compensation of lower temperature and larger volume, as well as the duality of hadronic and QGP rates). We also note that the inclusion of experimental acceptance cuts (*e.g.*, $p_{\rm t} > 0.2$ GeV and $y < 0.9$ for single electrons, representative of the cuts applied by STAR) noticeably distorts the proportionality between the low-mass excess radiation and fireball lifetime, as illustrated by the dotted line in Fig. 3. The main reason for this is that the increase of the transverse flow with collision energy lifts additional single-lepton tracks above the $p_{\rm t}$-cut into the detector acceptance. The proportionality of acceptance-corrected low-mass dilepton yields and the fireball lifetime is one of our main findings; it provides a promising tool to detect "anomalous" variations in the fireball lifetime which go beyond the, say, ∼ 20% level. A good control over the in-medium spectral shape turns out to be essential here, at the level established in the comparison to the NA60 data in Fig. 1.

In summary, we have computed thermal dilepton spectra in heavy-ion collisions over a wide range of collision energies, utilizing in-medium QGP and hadronic emission rates in connection with a lattice-QCD equation of state extrapolated to finite chemical potential. Our description satisfies the benchmark of the high-precision NA60 data at the SPS and is compatible with the recent results from the RHIC beam-energy scan. While systematic uncertainties due to the simplified space–time description in terms of our fireball model remain to be scrutinized, we believe that its successful phenomenology lends reasonable robustness to our study. Within this framework, we have extracted the excitation function of the low-mass excess radiation and the Lorentz-invariant slope of intermediate-mass spectra. The former turns out to accurately reflect the average fireball lifetime (and first tests from experiment are becoming available [57]). The latter signals QGP radiation well above $T_{\rm pc}$ at top RHIC energy, but closely probes the transition region for center-of-mass energies below 10 GeV. Dilepton radiation is thus well suited to provide direct information on the QCD phase boundary in a region where a critical point and an onset of a first-order transition are conjectured.

Acknowledgements

This work was supported in part by the U.S. National Science Foundation grant PHY-1306359, by the Humboldt Foundation (Germany), BMBF (Förderkennzeichen 05P12RFFTS) and LOEWE through the Helmholtz International Center for FAIR (HIC for FAIR).

References

[1] E.V. Shuryak, Phys. Lett. B 78 (1978) 150.
[2] G.E. Brown, M. Rho, Phys. Rev. Lett. 66 (1991) 2720.
[3] R.D. Pisarski, Phys. Rev. D 52 (1995) 3773.
[4] R. Rapp, J. Wambach, Adv. Nucl. Phys. 25 (2000) 1.
[5] M. Harada, K. Yamawaki, Phys. Rep. 381 (2003) 1.
[6] P. Braun-Munzinger, J. Stachel, C. Wetterich, Phys. Lett. B 596 (2004) 61.
[7] H. van Hees, C. Gale, R. Rapp, Phys. Rev. C 84 (2011) 054906.
[8] C. Shen, U.W. Heinz, J.F. Paquet, C. Gale, Phys. Rev. C 89 (2014) 044910.
[9] H. van Hees, M. He, R. Rapp, Nucl. Phys. A 933 (2015) 256.
[10] A. Adare, et al., PHENIX Collaboration, Phys. Rev. C 91 (2015) 064904.
[11] I. Tserruya, in: R. Stock (Ed.), Relativistic Heavy-Ion Physics, in: Landolt Börnstein (Springer), New Series, vol. I/23A, 2010, 4-2 arXiv:0903.0415 [nucl-ex].
[12] H.J. Specht, et al., NA60 Collaboration, AIP Conf. Proc. 1322 (2010) 1.
[13] R. Rapp, J. Wambach, Eur. Phys. J. A 6 (1999) 415.
[14] R. Rapp, E.V. Shuryak, Phys. Lett. B 473 (2000) 13.
[15] S. Borsanyi, et al., Wuppertal–Budapest Collaboration, J. High Energy Phys. 1009 (2010) 073.
[16] P.V. Ruuskanen, Nucl. Phys. A 525 (1991) 255.
[17] U.W. Heinz, K.S. Lee, Phys. Lett. B 259 (1991) 162.
[18] P. Roy, S. Sarkar, J. Alam, B. Dutta-Roy, B. Sinha, Phys. Rev. C 59 (1999) 2778.
[19] H. van Hees, R. Rapp, Nucl. Phys. A 806 (2008) 339.
[20] F. Geurts, et al., STAR Collaboration, Nucl. Phys. A 904–905 (2013) 217c.

[21] L. Adamczyk, et al., STAR Collaboration, Phys. Rev. Lett. 113 (2014) 022301.
[22] P. Huck, et al., STAR Collaboration, Nucl. Phys. A 931 (2014) 659.
[23] R. Rapp, Adv. High Energy Phys. 2013 (2013) 148253.
[24] S. Endres, H. van Hees, J. Weil, M. Bleicher, Phys. Rev. C 91 (2015) 054911.
[25] S. Endres, H. van Hees, J. Weil, M. Bleicher, Phys. Rev. C 92 (2015) 014911.
[26] B. Friman, C. Höhne, J. Knoll, S. Leupold, J. Randrup, R. Rapp, P. Senger, Lect. Notes Phys., vol. 814, 2011, 980 pp.
[27] M.A. Stephanov, PoS LAT 2006 (2006) 024.
[28] L.D. McLerran, T. Toimela, Phys. Rev. D 31 (1985) 545.
[29] H.A. Weldon, Phys. Rev. D 42 (1990) 2384.
[30] C. Gale, J.I. Kapusta, Nucl. Phys. B 357 (1991) 65.
[31] M. Urban, M. Buballa, R. Rapp, J. Wambach, Nucl. Phys. A 641 (1998) 433.
[32] R. Rapp, Phys. Rev. C 63 (2001) 054907.
[33] M. Dey, V.L. Eletsky, B.L. Ioffe, Phys. Lett. B 252 (1990) 620.
[34] J.V. Steele, H. Yamagishi, I. Zahed, Phys. Lett. B 384 (1996) 255.
[35] H.-T. Ding, et al., Phys. Rev. D 83 (2011) 034504.
[36] B.B. Brandt, A. Francis, H.B. Meyer, H. Wittig, J. High Energy Phys. 1303 (2013) 100.
[37] J.I. Kapusta, P. Lichard, D. Seibert, Phys. Rev. D 44 (1991) 2774;
J.I. Kapusta, P. Lichard, D. Seibert, Phys. Rev. D 47 (1993) 4171 (Erratum).
[38] E. Braaten, R.D. Pisarski, T.-C. Yuan, Phys. Rev. Lett. 64 (1990) 2242.
[39] I. Ghisoiu, M. Laine, J. High Energy Phys. 1410 (2014) 83.
[40] L. Kumar, et al., STAR Collaboration, arXiv:1408.4209 [nucl-ex].
[41] M. He, R.J. Fries, R. Rapp, Phys. Rev. C 85 (2012) 044911.
[42] S. Borsanyi, et al., J. High Energy Phys. 1011 (2010) 077.
[43] M. Cheng, et al., Phys. Rev. D 81 (2010) 054504.
[44] G. Endrodi, Z. Fodor, S.D. Katz, K.K. Szabo, J. High Energy Phys. 1104 (2011) 001.
[45] O. Kaczmarek, et al., Phys. Rev. D 83 (2011) 014504.
[46] S. Borsanyi, et al., J. High Energy Phys. 1208 (2012) 053.
[47] P. Hegde, et al., arXiv:1408.6305 [hep-lat].
[48] P. Braun-Munzinger, J. Stachel, arXiv:1101.3167 [nucl-th].
[49] R. Arnaldi, et al., NA60 Collaboration, Eur. Phys. J. C 61 (2009) 711.
[50] G. Agakichiev, et al., CERES Collaboration, Eur. Phys. J. C 41 (2005) 475.
[51] T. Renk, J. Ruppert, Phys. Rev. C 77 (2008) 024907.
[52] K. Dusling, D. Teaney, I. Zahed, Phys. Rev. C 75 (2007) 024908.
[53] J.K. Nayak, et al., Phys. Rev. C 85 (2012) 064906.
[54] O. Linnyk, E.L. Bratkovskaya, V. Ozvenchuk, W. Cassing, C.M. Ko, Phys. Rev. C 84 (2011) 054917.
[55] R. Rapp, PoS CPOD 2013 (2013) 008.
[56] A. Adare, et al., PHENIX Collaboration, arXiv:1509.04667 [nucl-ex].
[57] L. Adamczyk, et al., STAR Collaboration, Phys. Lett. B 750 (2015) 64.